International Journal of Thermophysics, Vol. 11, No. 3, 1990

Measurement of Optical Properties of Highly Scattering Ceramic Materials

S. S. Moiseev,[1] V. A. Petrov,[1] and S. V. Stepanov[1]

Received July 3, 1989

Radiation transfer in highly scattering ceramics is described by a diffusion approximation based on the asymptotic relation of the radiant flux and the radiant energy density in material depth. In this approximation, a calculation of the effective absorption coefficient k and the radiation diffusion coefficient D is based on the measurement of normal-hemispherical transmission of specimens shaped as various-thickness disks. Taken into account are radiation field, two-dimensionality, and the radiation boundary reflection effect. The optical property measurements have been performed on the experimental apparatus based on an integrating sphere, a collimated radiation source, and a two-channel data acquisition and processing system. Results of the measurements of k and D for the silica ceramic are given at room temperature.

KEY WORDS: absorption; ceramics; diffusion approximation; optical properties; radiation; scattering; transmittance.

1. INTRODUCTION

A calculation of temperature distribution and heat transfer in highly scattering dielectrics (e.g., ceramics, powders, and fibrous thermal insulations) must account for a combined energy transfer by radiation and heat conduction. Since the description of the radiation field for the above materials is difficult, the present approaches consist in finding either approximate solutions or asymptotics that correspond to an optically thick layer limit.

Depending on an inverse problem setup, various characteristics are used as material's volumetric optical properties. In the Gurevitch–Kubelka–Munk (GKM) theory [1–6] (the two-flux theory for diffused illumination), there are the K and S parameters, which represent, respec-

Institute for High Temperatures, USSR Academy of Sciences, Moscow 127412, USSR.

0195-928X/90/0500-0587$06.00/0

tively, diffuse absorption and diffuse back-scattering coefficients of a flat layer of unity thickness. A similar concept is expressed by Duntley's parameters [7, 8] in the four-flux theory for a directed illumination. It implies that the angle dependence of the radiation intensity in positive and negative hemispheres are similar and do not depend on the coordinates.

When an inverse problem is solved by the two- and four-flux methods within the transfer equation framework [3, 8–13], the unknown optical parameters are absorption coefficient k and scattering coefficient β, while the phase function is assumed to be known. However, the transfer equation is not valid for ceramic-type materials where distances between structural nonuniformities are comparable to the wavelength.

As is shown in Ref. 14 GKM two-flux methods in the limit

$$\begin{cases} \omega \to 1 \\ (k+\beta)L \to \infty \end{cases}$$

where $\omega = \beta/(k+\beta)$ is the albedo for scattering, and L is the thickness of the flat layer, fail to produce asymptotically accurate results, which restricts their applicability to solve inverse problems.

Diffusion methods [11, 14–18] are the most acceptable in describing the radiative transfer in optically thick layers of the scattering material. These methods are based on Fick's law for radiation diffusion which accurately correlates (asymptotically) radiation flux and radiant energy density in highly scattering material depth even for the cases when the transfer equation ceases to be valid. As shown in Ref. 18, application of the diffusion method for

$$\begin{cases} k D \to 0 \\ L/D \to \infty \end{cases}$$

limit produces asymptotically accurate expressions for bihemispherical reflectance (R_h), transmittance (P_h), and hemispherical absorptance (emittance) (ε_h) of a ceramic flat layer having thickness L and radiation diffusion coefficient D.

2. THEORY OF MEASUREMENTS

The present discussion is concerned only with highly diffuse low-absorption ceramics where conditions corresponding to the above-mentioned diffusion limit occurs at a distance within about 1 mm from the boundary. Normally, this corresponds to a rather wide spectral region between the electron absorption long-wave edge and the first fundamental atomic vibration band short-wave edge.

Reflectance of the flat layer for a such class of materials shows weak dependence on k and D, so the method used to determine these parameters is based on transmittance measurements. The precision of the determination of k based on experimental data for the transmittance is shown to be significantly dependent on whether optically thick [relative to attenuation coefficient $Z=(k/D)^{1/2}$] specimens are used for the measurements. For weak-absorption materials k may have the value of several thousands of cm^{-1}, which requires a flat layer thickness of several centimeters. The impossibility to realize an infinite flat layer of such thickness in performing transmittance measurements in an integrating sphere is evident. Consequently, the method used was based on the solution of an inverse problem of radiation diffusion for a disk-shaped specimen in the two-dimensional case.

We refer to the energy fractions (relative to the external diffuse radiation incident on face 1) coming from faces 1 and 2 as cylindrical specimen bihemispherical reflectance (R_h) and transmittance (P_h), respectively. The fraction of energy coming from the lateral surface is referred to as lateral bihemispherical transmittance ($P_{h,lat}$). Then, using the solution for energy density in a cylinder given in Ref. 19, one obtains

$$R_h(L,\rho_0)=1-\frac{16n^2D\rho_0}{\rho_b}\sum_{j=1}^{\infty}\frac{C_jZ_j}{X_j^2}[1+Z_jh_2+(1-Z_jh_2)-f_j^2] \quad (1)$$

$$P_h(L,\rho_0)=\frac{32n^2D\rho_0}{\rho_b}\sum_{j=1}^{\infty}\frac{C_jZ_jf_j}{X_j^2} \quad (2)$$

$$P_{h,lat}(L,\rho_0)=\frac{16n^2D}{\rho_0\rho_b}\sum_{j=1}^{\infty}\frac{C_j}{Z_j}[1+Z_jh_2+(1-Z_jh_2)f_j^2-2f_j] \quad (3)$$

$$\varepsilon_h(L,\rho_0)=\frac{16n^2k\rho_0}{\rho_b}\sum_{j=1}^{\infty}\frac{C_j}{Z_jX_j^2}[1+Z_jh_2+(1-Z_jh_2)f_j^2-2f_j] \quad (4)$$

where

$$C_j=\frac{J_1(X_j\rho_b/\rho_0)}{J_1(X_j)(1+h_{lat}^2X^2/\rho_0^2)[(1+Z_jh_1)(1+Z_jh_2)-(1-Z_jh_1)(1-Z_jh_2)f_j^2]}$$

$$f_j=\exp(-Z_jL); \qquad Z_j=(Z^2+X_j^2/\rho_0^2)^{1/2};$$

$$h_{lat}=2D(1+r_{h,lat})/(1-r_{h,lat}); \quad (5)$$

ρ_0 is the radius of the cylinder; ρ_b is the radius of the spot produced by the external diffuse radiation incident of face 1; $h_i=2D(1+r_{hi})/(1-r_{hi})$ and r_{hi} $(i=1,2)$ are the bihemispherical boundary internal reflection coefficients, where the value $i=1$ relates to flat boundary 1 on which the radiation is

incident, and $i=2$ relates to boundary 2; $r_{\mathrm{h,lat}}$ is the bihemispherical boundary internal reflection coefficient for the lateral surface; n^2 is the volume mean (allowing for porosity) refractive index squared; k is the effective absorption coefficient [20]; and X_j is the root of the following characteristic equation:

$$J_0(X) - (Xh_{\mathrm{lat}}/\rho_0)\, J_1(X) = 0 \tag{6}$$

where $J_0(X)$ and $J_1(X)$ are the Bessel functions of zero and first orders, respectively. It may be noted that great variations in r_{hi} values produce only small changes in k and D, which makes it sufficient to use a rather coarse reflection model. This is significant, since generally reflective characteristics are not well known (except for the polished-boundary case). In this paper the material–air flat boundary was represented as a set of air–air and solid matrix–air fragmented boundaries. It is this model that was used to calculate the r_{hi} coefficients.

Equation (2) provides a theoretical basis for the method of determining absorption and diffusion coefficients in a two-dimensional case. However, it also requires diffuse illumination of cylindrical specimen face 1, which is somewhat complicated in practice. This difficulty may be bypassed if the problem is reduced to the directional-hemispherical transmission using parallel falling radiation beam. Since the angular distribution of the transmitted radiation within the diffusion limit depends neither on the specimen radius and thickness nor on the direction if the incident radiation, bidirectional transmittance can be expressed by

$$P(L, \rho_0, \Omega, \Omega') = U(\Omega) \cdot P(L, \rho_0, \Omega')/\pi \tag{7}$$

where Ω is the point on the surface of a unity-radius positive hemisphere defined by location angle $\theta \in [0, \pi/2]$ and azimuth $\varphi \in [0, 2\pi]$; the third argument in the expression corresponds to the transmitted radiation direction; the fourth, to the incident; $P(L, \rho_0, \Omega)$ is the directional-hemispherical transmittance (i.e., transmission coefficient); and $U(\Omega)$ is the transmission phase function normalized in accordance with the following equation:

$$\int_{(2\pi)} U(\Omega)\mu \, d\Omega = \pi \tag{8}$$

where $\mu = \cos\theta$.

It is easy to demonstrate that normal hemispherical transmission coefficient $P_n(L, \rho_0) = P(L, \rho_0, \mu = 1)$ is equal to

$$P_n(L, \rho_0) = U_n P_h(L, \rho_0) \tag{9}$$

where $U_n \equiv U(\mu = 1)$. The value of $U(\Omega)$ is a function normalized by the condition of Eq. (8), while in the experiment a nonnormalized angular dependence $\tilde{U}(\Omega)$ may be measured, which is a radiation detector signal proportional to the energy coming from face 2 into the integrating sphere at various turns of the specimen relative to the incident collimated radiation. It is obvious that $U(\Omega) = a\tilde{U}(\Omega)$, where, using Eq. (8), we find

$$a = \pi \Big/ \int_{(2\pi)} \tilde{U}(\Omega)\mu \, d\Omega$$

or

$$U_n = \pi \tilde{U}_n \Big/ \int_{(2\pi)} \tilde{U}(\Omega)\mu \, d\Omega \tag{10}$$

where $\tilde{U}_n \equiv \tilde{U}$ $(\mu = 1)$. If the layer is azimuth-symmetrical (only an azimuthal symmetry of the specimen material and boundary 1 is required in practice), then $U(\Omega) = U(\theta)$, and

$$U_n = \tilde{U}_n \Big/ \left(2 \int_0^1 \tilde{U}(\mu)\mu \, d\mu \right) \tag{11}$$

Equations (2), (9), (10), and (11) are the working relations of the method that allow to substitute solution of an inverse radiation transfer problem for diffuse incident radiation to that for collimated incidence.

3. EXPERIMENTAL METHOD AND APPARATUS

The first phase of the experiment is to determine the function $\tilde{U}(\Omega)$ and to calculate U_n on the basis of Eq. (11). The second phase involves measurement of transmittance of specimens with various thicknesses for normal incident collimated radiation and obtaining k and D values that, as far as the least-squares method (LSM) is concerned, are the best to approximate the experimental results by means of Eq. (9)-type functions.

Measurements at both phases were performed with the same apparatus, using similar methods that differed only in specimen mounting techniques. Additional measurements related to the reference mounting were performed at the second phase.

The apparatus is shown in Fig. 1. Collimated radiation of laser 11 passes through disk modulator 12 and interference filter 13 and arrives at radiation dividing plate 14. The greater part of the radiation passes through the plate and is focused by lens 6 on specimen 7 mounted in holder 15. The specimen is positioned in the inlet of the integrating sphere

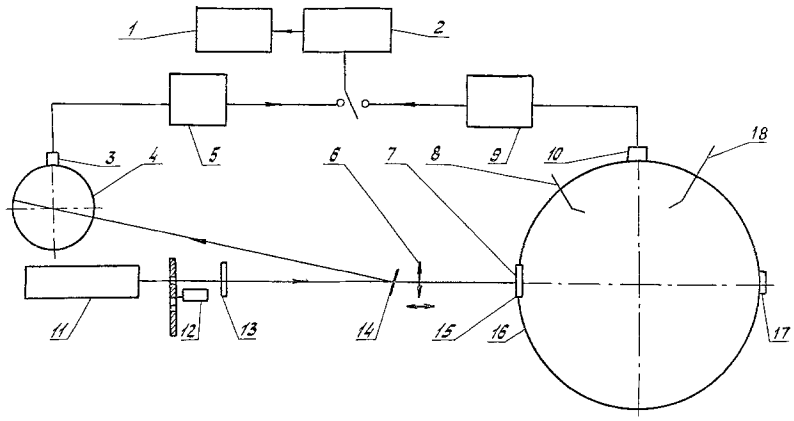

Fig. 1. The schematic of the apparatus.

of 200-mm diameter. Multiple reflections of radiation transmitted by the test specimen produces an even radiation distribution on the sphere's inner surface. Detector 10 is screened with shield 8 or 18 from falling of straight radiation transmitted by the test specimen or reflected by the reference specimen 17. Its signal is amplified by lock-in amplifier 9. The smaller part of the laser radiation reflected from the radiation dividing plate arrives at the small integrating sphere 4 of 100-mm diameter. This sphere contains detector 3 whose signal is also amplified by lock-in amplifier 5. This scheme allows the computer to introduce a correction for small changes in the intensity of the laser radiation over the time period between measurements on the test specimen transmission and reflection of reference specimen positioned in the sphere's outlet.

Main and auxiliary photometric channel signals are alternatively measured by digital voltmeter 2 connected to data acquisition and processing system 1 which includes a modular instrumentation system CAMAC and the computer.

Since an acceptable precision of k determination may be obtained only if the specimen used has an appreciable (relative to attenuation) thickness, measurements of small transmission values reaching 10^{-4}–10^{-5} are required. In this case reliability of the data obtained is provided by using lasers as high-power monochromatic radiation sources, selection and setting of the electronic circuits, and ensuring linearity of the detector and amplifier over an entire range of the signals being measured. Since $\tilde{U}(\Omega) \equiv \tilde{U}(\mu)$ does not depend on L, its measurement is carried out on one specimen of an arbitrary thickness.

The function $\tilde{U}(\mu)$ had been determined from measurement of detector

signals proportional to the laser energy transmitted by the specimen when incidence angles were 0, 10, 20,...,80, 88°. A required angle was set by rotation of the integrating sphere around its vertical axis and by corresponding displacement of the sphere in the plane perpendicular to the laser beam.

Measurement of normal-hemispherical transmittance involved comparison of the signals obtained in alternative placement of the test specimen and the reference specimen in the inlet and outlet of the integrating sphere, respectively. An opal glass specimen was used as the reference for the visible spectrum; a calcium fluoride ceramics, for the infra-red. Reflection of the references was known with an uncertainty of $\pm 1\%$.

4. RESULTS

The silica ceramic investigated was fabricated from a pure optical silica glass and had a porosity of 55.6%. Grain sizes ranged from one to tens of micrometers.

A specimen of $L = 4$ mm in thickness and $\rho_0 = 15$ mm in radius was used for the determination of the transmission phase function $\tilde{U}(\mu)$. The thickness selection was conditioned by two considerations: first, the signal from the radiation detector must be sufficiently large; and second, the radiation coming from the lateral surface of the specimen must be significantly smaller than that coming from face 2 (the one-dimensionality requirement).

The results obtained from transmission phase function measurements for the wavelengths 0.63 and 1.15 μm are satisfactorily approximated by the third-degree polynomials of the following form:

$$\tilde{U}(\mu)/U_n^2 = 0.306 + 1.001\,\mu - 0.358\,\mu^2 + 0.051\,\mu^3 \qquad (\text{for } \lambda = 0.63\ \mu\text{m})$$

$$\tilde{U}(\mu)/\tilde{U}_n = 0.270 + 0.877\,\mu - 0.138\,\mu^2 + 0.027\,\mu^3 \qquad (\text{for } \lambda = 1.15\ \mu\text{m})$$

Figure 2 shows the $U(\mu)$ as a function of angle θ calculated in accordance with the above relations.

Normal-hemispherical transmittance was measured on specimens with thicknesses ranging from 2 to 10 mm; several specimens of each thickness were used. Typical scatter of the transmittance value for specimens of the same thickness did not exceed 15% and was primarily caused by specimen structural nonuniformity. The random error was several times smaller; this is attributed to several measurements performed for each specimen.

Result processing carried out on the computer consisted of minimization of the function

$$F(k, D) = \sum_{m=1}^{N} W_m \sum_{j=1}^{N_m} [P_n(L_m, k, D) - P_{jm}]^2 \qquad (12)$$

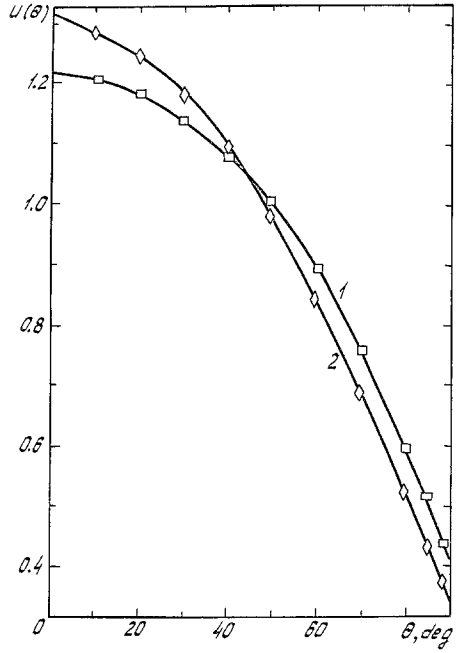

Fig. 2. Variation of the quantity $U(\mu)$ as a function of angle θ: curve 1, $\lambda = 0.63\ \mu$m; curve 2, $\lambda = 1.15\ \mu$m.

where P_{jm} are experimental transmittance values for a set of specimens of the thickness ($j \in \overline{1, N_m}$); m is the specimen number in the group of specimens having the same thickness ($m \in \overline{1, N}$); W_m is the measurement weight; and $P_n(L_m, k, D)$ are calculated transmittance values.

The values of k and D found by the above method for the silica ceramic investigated at room temperature, along with the confidence intervals for 95% confidence probability, are as follows:

$$k = (1.2 \pm 0.3)10^{-2}\ \text{cm}^{-1}; \qquad D = (8.7 \pm 0.8)10^{-4}\ \text{cm} \qquad (\lambda = 0.63\ \mu\text{m})$$

$$k = (7.9 \pm 0.5)10^{-3}\ \text{cm}^{-1}; \qquad D = (1.55 \pm 0.03)10^{-3}\ \text{cm} \qquad (\lambda = 1.15\ \mu\text{m})$$

It is important to know what k and D errors may be caused if one neglects angular dependence of directional-hemispherical transmission, i.e., if $P_n = P_h$ or $U_n = 1$ is assumed. If the boundary reflection coefficients are not close to unity, the values of k and D may be shown to be asymptotically inverse by proportional to U_n. So the fact that $U_n = 1.23$

($\lambda = 0.63\ \mu$m) and $U_n = 1.33$ ($\lambda = 1.15\ \mu$m) shows that a failure to account for angular dependence $P(\theta)$ leads to errors in the values of k and D which are equal to 23 and 33%, respectively.

5. CONCLUSION

The method developed for the determination of highly scattering low-absorption materials' optical properties on the basis of diffusion approximation allows one to describe a radiation field even when the transfer equation is not valid. The optical properties of such materials have been described in terms of two coefficients: the radiation diffusion coefficient D and the effective absorption coefficient k. The first depends on porosity, sizes of pores, and refractive index of the material and on it does not change much as the temperature is increased. The second depends on temperature much more.

In this paper we have presented results which were obtained at room temperature. However, the method may also be used at high temperatures.

REFERENCES

1. M. M. Gurevich, *Trudy Gosudarstvennogo Opt. Inst.* (Transactions of the State Optical Institute) **6**(57):1.20 (1931).
2. P. Kubelka and F. Munk, *Z. Techn. Phys.* **20**:593 (1931).
3. A. A. Gershun, *Trudy Gosudarstvennogo Opt. Inst.* (Transactions of the State Optical Institute) **11**(99):43 (1936).
4. J. C. Richmond, *J. Res. NBS* **67**:212 (1963).
5. W. A. Allen and A. J. Richardson, *JOSA* **58**:1023 (1968).
6. N. A. Voishvillo, *Opt. Spectrosk.* (Optics and Spectroscopy) **37**:136 (1974).
7. S. Q. Duntley, *JOSA* **32**:61 (1942).
8. P. S. Mudgett and L. W. Richards, *Appl. Opt.* **10**:1458 (1971).
9. S. G. Iliasov and V. V. Krasnikov, *Inzhenerno-fiz. Z.* (Physical Engineering Journal) **23**:267 (1972).
10. S. G. Iliasov and V. V. Krasnikov, *Fizicheskie osnovy infrakrasnogo oblucheniya pistchevyh productov* (Physical Basics of Food IR Treatment) (Moscow, 1978), pp. 86–111.
11. A. Isimaru, *Rasprostranenie i rasseyanie voln v sluchaino neodnorodnyh sredah* (Wave propagation and Scattering in Random Media) (Moscow, 1981), Vol. 1, pp. 195–211.
12. Z. A. Yasa and W. B. Jackson, *N. M. Am. Appl. Opt.* **21**:21 (1982).
13. J. Reichman, *Appl. Opt.* **12**:1811 (1973).
14. V. A. Petrov and S. V. Stepanov, *Izvest. SO AN SSSR Ser. Tech. Nauk* (The USSR Academy of Sciences, Siberian Branch News, Application Science Series) **2**(7):21 (1987).
15. Yu. A. Tsirlin, L. E. Pargamanik, and A. P. Daich, *Opt. Spectrosk.* (Optics and Spectroscopy) **12**:304 (1962).
16. L. F. Gate, *Appl. Opt.* **13**:236 (1974).

17. N. M. Bazhin and S. M. Baranov, *Opt. Spectrosk.* (Optics and Spectroscopy) **34**:963 (1973).
18. S. V. Stepanov and M. A. Berkovsky, *Teplofiz. Vysokih Temp.* (Thermophysics of High Temperatures) **23**:346 (1985).
19. M. A. Berkovsky and V. A. Stepanov, *Teplomassoobmen-VII, Vol. 2* (Institute of Mass and Heat Transfer, Minsk, 1984), pp. 30–34.
20. S. V. Stepanov, *Teplofiz. Vysokih Temp.* (Thermophysics of High Temperatures) **25**:180 (1988).